Surface Characteristics Comparison of Machining Waste Using Powder Metallurgy Method

Ika Silviana Widianti[a], Yoga Kartiko Raharjo [a], Ahmat Safa'at[a], Suhariyanto[a], Giri Nugroho[a]*

[a]*Industrial Mechanical Engineering, Sepuluh Nopember Institute of Technology, Surabaya 60117, Indonesia*
Corresponding author: ika.widianti@its.ac.id

Abstract
Machining processes generate metal waste in the form of fine powder that is often not reused efficiently. This study explores the potential reuse of metal machining waste powder through powder metallurgy, focusing on how sintering temperature affects mechanical properties and microstructure. Metal powder from ST60 steel machining was compacted and sintered at 1100°C, 1150°C, and 1200°C. The specimens were then compared to original ST60 steel. XRF analysis confirmed that iron was the dominant element in the waste powder. Microstructural analysis showed the presence of ferrite and pearlite in all specimens, with higher sintering temperatures increasing the ferrite content. In terms of mechanical performance, ST60 steel showed the highest hardness (80.6 HRB) and compressive strength (156.157 N/mm²). Among the specimens, the one sintered at 1100°C had the highest hardness (65.1 HRB) and compressive strength (73.293 N/mm²), closest to ST60 steel. The lowest surface roughness (7.058 Ra) was observed in the 1200°C specimen, approaching ST60's value (2.003 Ra). These findings indicate that reused machining waste powder can be processed into useful products, especially for low-load applications, with optimal properties achieved at 1100°C sintering temperature.

Keywords: Machining waste; Mechanical properties; Powder metallurgy; Sintering; ST60 steel

1. Introduction

Indonesia, as a developing country, is committed to improving the welfare of its people through development in various sectors, including science and technology. Advancements in science and technology have contributed to the growth of the manufacturing industry in Indonesia[1], as reflected in the increased production rates in this sector. In support of enhanced production capabilities, machine tools play a vital role. However, machining processes often produce metal residues[2] that result in waste materials such as chips and bursts. Improper handling of this waste materials can negatively impact on the surrounding environment.

Chips are generated during the cutting process of a workpiece using cutting tools or machine tools[2]. They are typically irregular in shape and include fine metal particles. Burs, on the other hand, are formed during the deburring process, which involves removing residual metal and smoothing the workpiece surface. Burs are usually composed of unused metal particles. Thus, both chips and burs are by-products of machining processes in the form of metal powder[1], [2]. Metal powders are significantly more expensive than solid metals[3] and are generally reserved for mass production due to their higher processing costs. Therefore, proper handling and treatment of these metal powders are crucial to converting them into value-added products. Powders with small particle sizes and spherical shapes are especially suitable for Powder Metallurgy (PM)[4] methods due to their ability to produce low-porosity components.

Powder Metallurgy is widely utilized in material fabrication. It is a process that forms commercial workpieces (either finished or semi-finished) from metal powders[5]. In this method, the powders are compacted in a mold and then heated below their melting point[6], allowing the particles to bond through mass transport mechanisms induced by atomic diffusion at the particle interfaces[3].

This study investigates the elemental composition[7] of the resulting metal powders and examines the effects of sintering temperature on the microstructure and mechanical properties of the compacted specimens[8], [9], [10], [11].

2. Method

2.1. Flowchart

Overall, the experimental procedures in this final project are presented in the form of the flowchart shown below

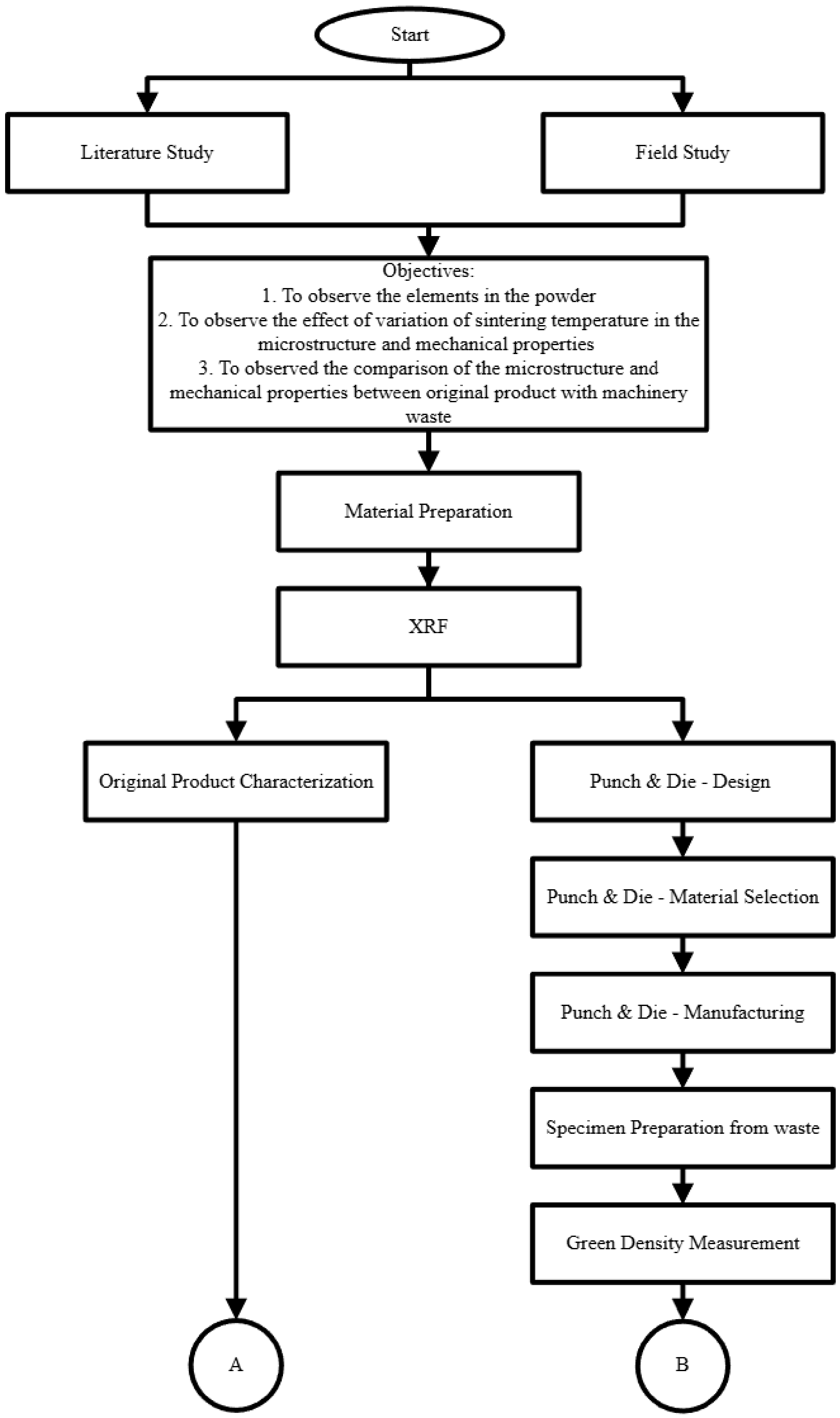

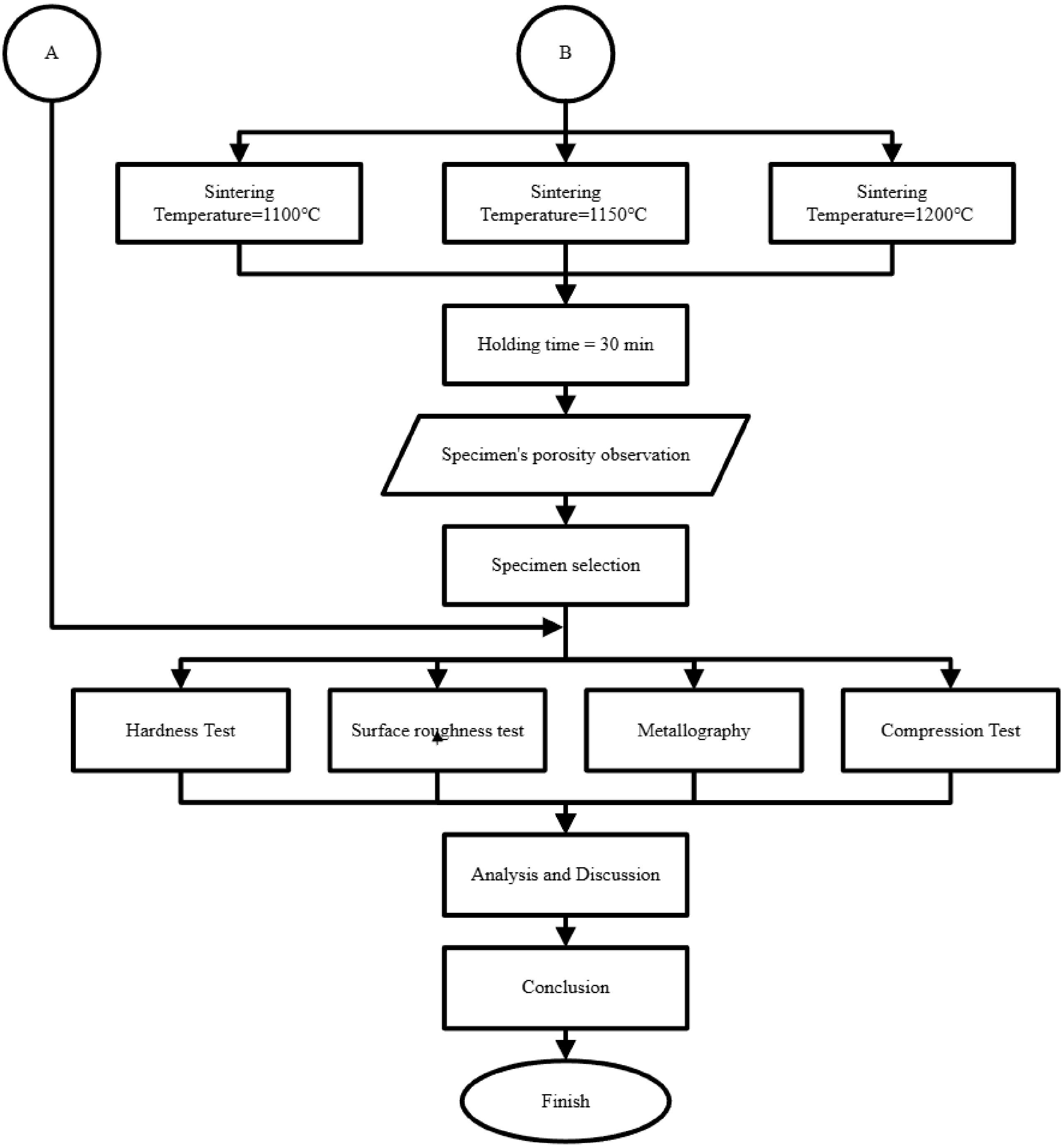

Figure 1. Experiment flowchart

2.2. Materials

The primary material used in this study was machining waste chips[3], [12], serving as the main component. Zinc stearate was used as both a lubricant and a binder[6], [13]. Shaft steel was utilized as the material for the fabrication of punches and dies[14]. The original product material, ST60 steel[15], was used as a reference for comparing the mechanical properties of the test specimens[1], [2].

2.3. Powder Collection

The chips were collected from various machining processes, preferably from ST60 steel. The target was to obtain a homogeneous powder. Therefore, a sieving process[5] was conducted using a Test Sieve with Mesh 100 and an aperture size of 0.149 mm[16].

Figure 2. a) Machining waste, b) Test sieve mesh 100, c) Powder after sieving.

2.4. Powder Mixing Using Dry Mixing Method

In preparing the specimens, a powder mixture consisting of 97.5% iron (Fe) and 2.5% zinc stearate was used, corresponding to 20.5 grams of Fe and 0.5 grams of zinc stearate, resulting in a total initial mass of 21 grams[17]. Zinc stearate served as both lubricant and binder in the mixture. Before mixing, the Fe powder appeared dark grey, and after mixing with zinc stearate, it appeared light grey. The mixing process plays a crucial role in the compacting outcome[18].

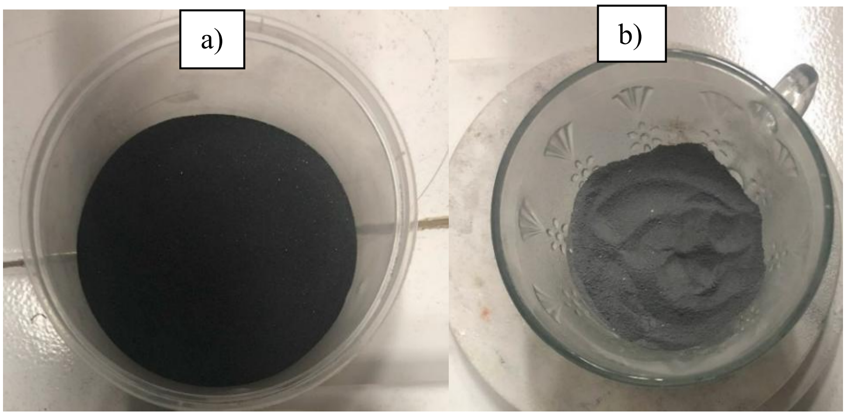

Figure 3. a) Powder before mixing with zinc stearate and b) Powder after mixing with zinc stearate.

2.5. Punch and Die Design

Specimens were designed with a diameter and height of 20 mm. The punch and die were designed using Autodesk Inventor software[19] and fabricated using a lathe from shaft steel. The fabricated punch measured 70 mm in total height with a 20 mm diameter pressing section. The collected powder was used to produce three specimens using the punch and die setup, followed by compaction and sintering.

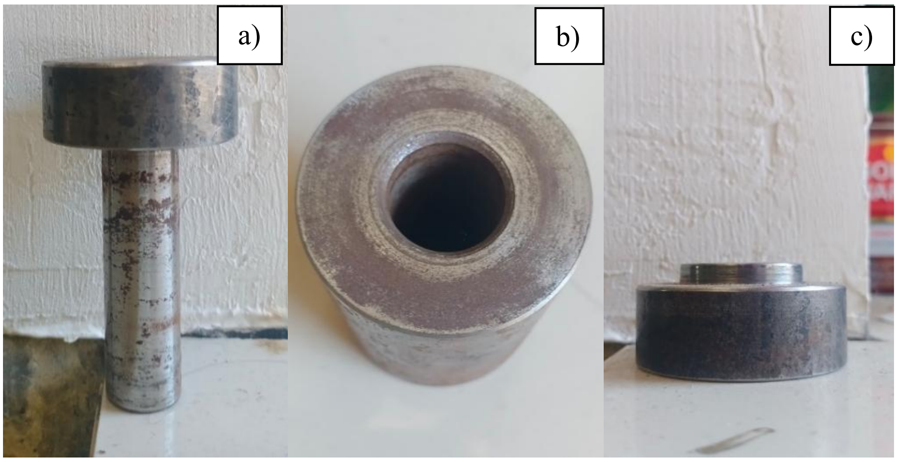

Figure 4. Design of a) punch, b) die, and c) support holder.

2.6. *Compaction*

Prior to compaction, the powder was mixed with zinc stearate to reduce porosity and facilitate ejection from the mold. The compaction was carried out under a pressure of 400 MPa[20] using a compaction device[21], followed by measurement of the green density. Green density refers to the ratio of the compacted powder's volume to its external volume and indicates how densely the particles are packed. The average green density of the three compacted specimens was 3.62 g/cm³. The compaction process increased the density as higher compaction pressure resulted in closer particle packing, reduced porosity, and increased material density.

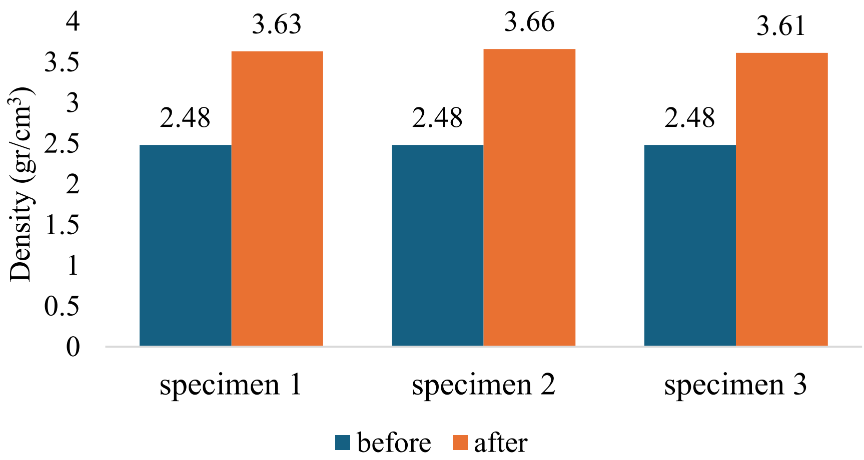

Figure 5. Density value comparison of before and after compaction.

2.7. *Sintering*

Sintering is a manufacturing process used to produce solid components from powders or granules, commonly composed of metals, ceramics, or other materials. In this stage, the specimens obtained from the compaction process were subjected to three different heat treatment temperatures: 1100°C, 1150°C, and 1200°C.

Based on the comparison of density after sintering, all three specimens exhibited a decrease in density. The results indicate that the higher the sintering temperature, the lower the resulting density of the specimens. This phenomenon can be attributed to the significant influence of sintering temperature on the shape and size of the specimens. At higher temperatures, the specimens tend to exhibit a semi-molten appearance, leading to dimensional changes and an increase in overall volume.

An increase in sintering temperature can promote grain boundary growth between particles, which results in shrinkage of the specimen structure. This occurs as larger particles begin to coalesce and rearrange the powder configuration, leading to reduced packing density.

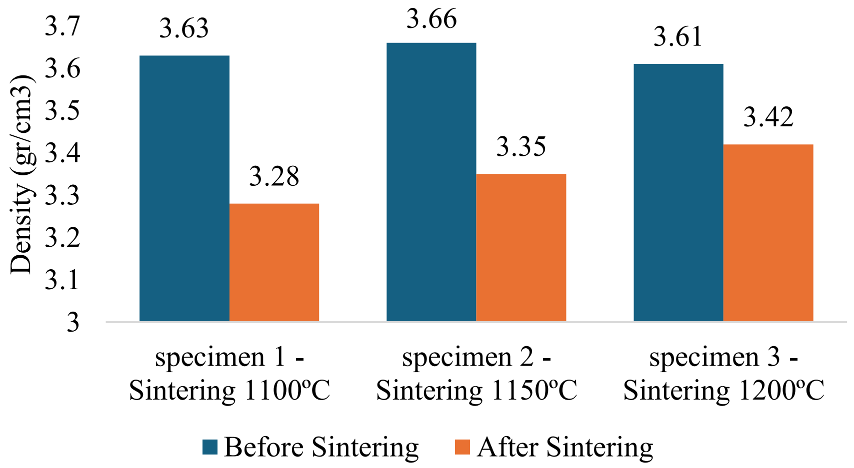

Figure 6. Density value comparison of before and after sintering.

3. Results and Discussion

3.1 Chemical Composition of ST60 and Chip Specimen

The reference material used for comparing the test specimens was ST60 steel, as it was one of the materials used during the machining process. The metal chips collected from the machining waste were analyzed using X-Ray Fluorescence (XRF)[7] to determine the elemental composition. The XRF analysis revealed that iron (Fe) was the dominant element in the machining waste powder, with a concentration of 82.53%, compared to 98.51% in the ST60 steel. Other elements identified in the powder, which were also present in ST60 steel, included phosphorus, carbon, ferrum, manganese, and sulfur, indicating some compositional similarity between the waste powder and the reference material.

Table 1. XRF results between ST60 and Chip specimen

Elements	Chip specimen	ST60	Unit
Al	0.7	-	%
Si	3	-	
Ca	1.5	-	
P	0.3	0.04	
S	0.3	0.05	
K	0.2	-	
C	0.08	0.5	
Ti	8.9	-	
V	0.43	-	
Cr	0.47	-	
Mn	0.77	0.8	
Fe	82.53	98.51	
Ni	0.27	-	
Cu	0.091	-	
Zn	0.086	-	
Rb	0.02	-	

Zr	0.04	-
Mo	0.15	-
Re	0.05	-
Bi	0.09	-

3.2 Non-Destructive Testing of Specimens and ST60

A. Porosity testing

Porosity testing was conducted to evaluate the void spaces within the material[22]. The porosity of the specimens was analyzed using ImageJ software. Results showed that porosity tends to decrease with increasing sintering temperature. This is due to stronger bonding between powder particles at higher temperatures, which reduces the gaps between them. Lower porosity indicates fewer voids and improved material integrity.

A comparison with the reference ST60 material, which had the lowest porosity at 2.814%, showed that the specimen sintered at 1200°C had a porosity of 9.892%, the lowest among the sintered specimens. Although higher than ST60, this value reflects a significant reduction in porosity as sintering temperature increases.

Table 2. Summary of Software ImageJ Measurement

Name	Count	Average size	%Area
ST60	257	18	2.81
Spesimen 1 Sintering 1100ºC	338	49.81	14.35
Spesimen 2 Sintering 1150ºC	1136	10.76	10.93
Spesimen 3 Sintering 1200ºC	815	10.10	9.89

B. Metallographic analysis

Prior to metallographic analysis[23], the specimens were surface-ground and polished to ensure a clear observation of microstructures. The analysis was conducted at magnifications of 100x to 200x. The microstructure observations revealed the presence of pearlite and ferrite phases in both ST60 and the sintered specimens.

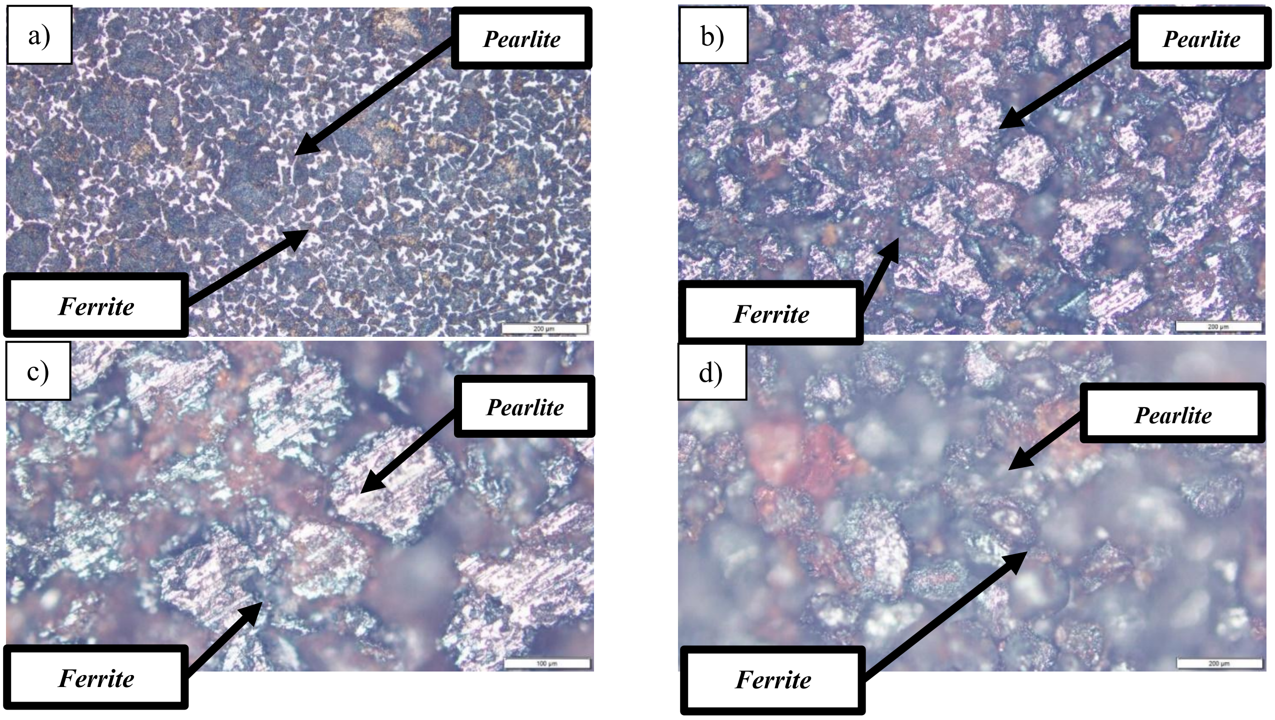

Figure 7. Microstructures of (a) ST60, (b) sintered at 1100°C, (c) 1150°C, (d) 1200°C.

The appearance of pearlite and ferrite in all specimens is attributed to exposure to elevated temperatures followed by air cooling (normalizing). In the micrographs, pearlite appears dark and lamellar, while ferrite appears white and equiaxed. As the sintering temperature increases, the amount of pearlite decreases, indicating a phase transformation [24]. This reduction in pearlite content can negatively affect the mechanical properties of the material, as pearlite is harder and stronger than ferrite, which is softer and more ductile.

C. Surface Roughness testing

Surface roughness was measured using the Mitutoyo SJ-210 surface roughness tester[16], [22] to determine the finish of the specimens after sintering. The data showed a decreasing trend in roughness with increasing sintering temperature.

- specimen 1 - Sintering 1100°C, the average surface roughness (Ra) from three measurement points was 13.618 µm.
- specimen 2 - Sintering 1150°C, the roughness decreased to 9.937 µm.
- specimen 3 - Sintering 1200°C, it further decreased to 7.058 µm.

This inverse relationship between sintering temperature and surface roughness suggests that higher sintering temperatures promote particle fusion, reduce porosity, and enhance atomic diffusion, leading to smoother surfaces.

3.3 Destructive Testing of Specimens and ST60

A. Hardness testing

Hardness testing was conducted using the Rockwell B (HRB) scale[22], employing a 1/16" steel ball indenter. This type of indenter was selected to minimize damage to the brittle specimens. The results showed a decreasing trend in hardness values with increasing sintering temperatures:

- ST60 reference: 80.6 HRB
- specimen 1 - Sintering 1100°C: 65.1 HRB
- specimen 2 - Sintering 1150°C: 59.8 HRB
- specimen 3 - Sintering 1200°C: 58.47 HRB

The decline in hardness is attributed to the microstructural evolution toward a more ferrite-dominant phase at higher temperatures. Since ferrite has lower hardness and higher ductility compared to pearlite, the mechanical strength of the material decreases as ferrite content increases.

B. Compression testing

Compression testing was performed to evaluate the compressive strength of the specimens. The cross-sectional areas were as follows:

- ST60: 314 mm²
- specimen 1 - Sintering 1100°C: 307.75 mm²
- specimen 2 - Sintering 1150°C: 304.54 mm²
- specimen 3 - Sintering 1200°C: 301.57 mm²

The highest compressive strength was observed in the ST60 reference specimen at 156.157 N/mm². The sintered specimens exhibited the following values:

- specimen 1 - Sintering 1100°C: 73.29 N/mm²
- specimen 2 - Sintering 1150°C: 57.94 N/mm²
- specimen 3 - Sintering 1200°C: 29.27 N/mm²

This decreasing trend is consistent with the increasing ferrite content at higher sintering temperatures. As ferrite has lower strength compared to pearlite, the overall compressive strength of the specimens declines with the transformation of the microstructure.

3.4 Correlation Between Tests

A. Correlation Between Porosity and Surface Roughness

Surface roughness refers to the measure of irregularities or deviations on the surface texture of a specimen. A higher roughness value typically indicates the presence of more pronounced peaks and valleys on the surface.

Meanwhile, porosity refers to the volume fraction of voids within the material. High porosity indicates a larger amount of internal empty space.

Table 3. Correlation between porosity and surface roughness.

Name	Porosity (%)	Surface Roughness (Ra)
ST60	2.81	2.003
Spesimen 1 - Sintering 1100ºC	14.35	13.618
Spesimen 2 - Sintering 1150ºC	10.93	9.937
Spesimen 3 - Sintering 1200ºC	9.89	7.058

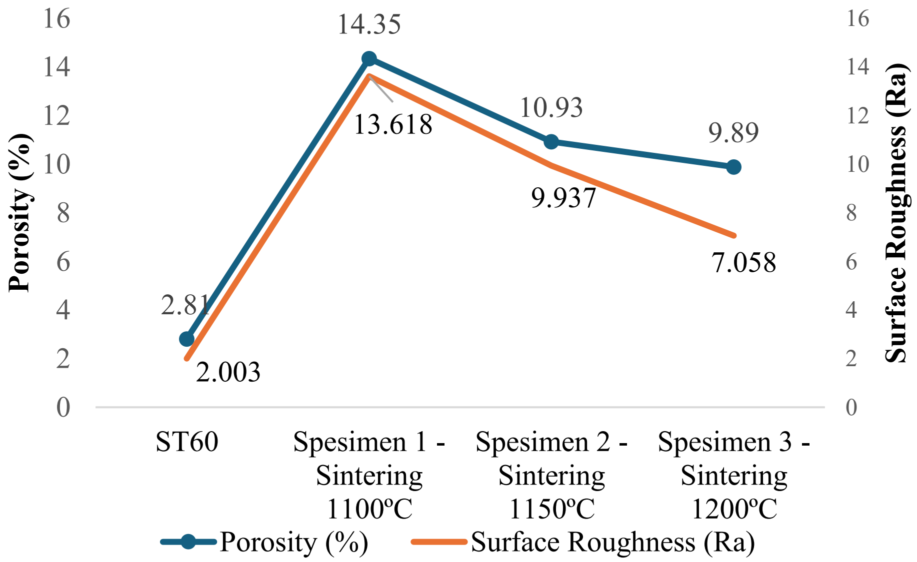

Figure 8. Graphic correlation between porosity and surface roughness.

The results suggest that as porosity decreases, surface roughness also tends to decrease. This indicates a strong correlation where improved particle bonding at higher sintering temperatures contributes to both reduced porosity and a smoother surface finish. Therefore, increased sintering temperature positively influences both densification and surface quality, resulting in materials with improved integrity and finish.

B. Correlation Between Hardness, Compressive Strength, and Metallography

Both hardness and compressive strength were observed to decrease with increasing sintering temperatures. This trend indicates that elevated sintering temperatures may lead to a reduction in the mechanical performance of the material. Metallographic observations revealed that as sintering temperature increased, the resulting microstructure became increasingly dominated by ferrite.

Table 4. Correlation between hardness and compressive strength.

Name	Hardness value (HRB)	Compressive strength (N/mm^2)
ST60	80.6 HRB	156.157
Spesimen 1 - Sintering 1100ºC	65.1 HRB	73.293
Spesimen 2 - Sintering 1150ºC	59.8 HRB	57.941
Spesimen 3 - Sintering 1200ºC	58.47 HRB	29.266

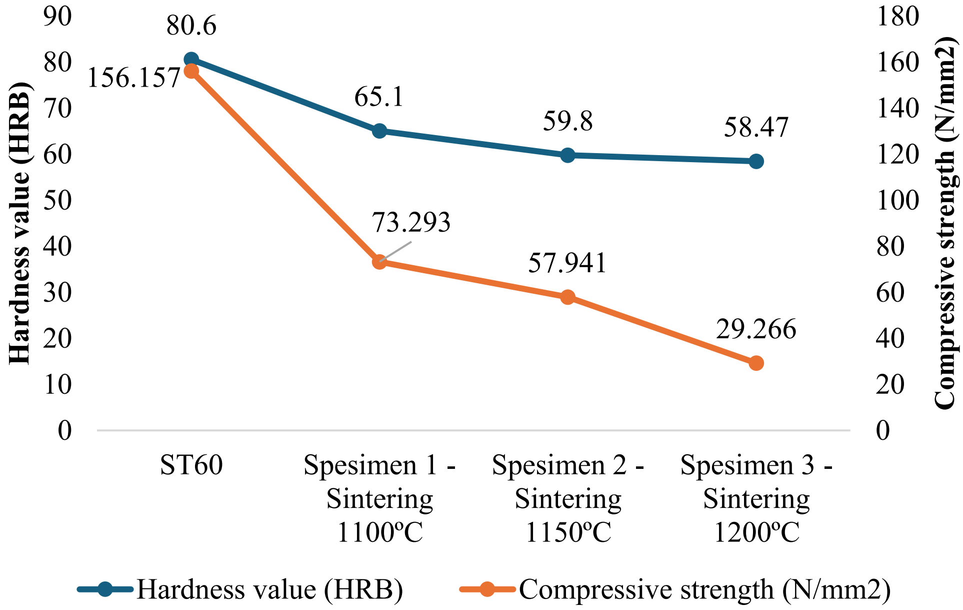

Figure 9. Graphic correlation between hardness and compressive strength.

This shift in microstructure significantly influences the mechanical properties, as ferrite is known to be softer and more ductile compared to pearlite. The prevalence of ferrite at higher temperatures contributes to the observed decline in both hardness and compressive strength.

Therefore, optimizing the sintering temperature is essential to achieve a desirable balance between mechanical properties such as hardness and compressive strength, while managing microstructural transformations effectively.

3.5 Application

Based on the results and discussions presented, the processed specimens show potential for practical applications in the form of useful and functional components. Given the mechanical characteristics obtained, particularly the relatively lower strength and hardness, the specimens are best suited for applications that do not involve dynamic or high-load stresses.

Hence, these materials can be applied in static components such as door handles, table legs, window handles, and motorcycle footrests. These applications require dimensional stability and adequate surface quality but not high mechanical strength. As such, the specimens can be developed into value-added products for non-structural or lightly loaded applications

4. Conclusions

According to the discussion above, it can be concluded that:

1. The elemental composition of metal chips obtained from machining waste was successfully identified using X-Ray Fluorescence (XRF) analysis. The dominant element detected in the powder was iron (Fe), with a concentration of 82.53%. The powder used in this study was sieved to a particle size of 100 mesh.
2. Sintering temperature has an inverse correlation with the mechanical properties of the specimens. As the sintering temperature increases, both hardness and compressive strength decrease. Higher sintering temperatures lead to greater shrinkage of the specimens, resulting in a reduction in height and volume changes. Elevated temperatures also reduce porosity due to enhanced particle bonding and densification, which contributes to lower surface roughness values. In terms of microstructure, the specimens predominantly exhibited ferrite and pearlite phases. As sintering temperature increases, the proportion of pearlite decreases while ferrite increases. This shift leads to a decline in mechanical strength, as ferrite is softer and more ductile than pearlite.
3. The comparison of microstructures between ST60 steel and the sintered specimens revealed similar phase formation, namely pearlite and ferrite. However, in terms of mechanical performance, ST60 steel demonstrated

superior hardness and compressive strength compared to all three sintered specimens. Among the specimens, the one sintered at 1100°C exhibited mechanical properties most closely resembling those of ST60 steel. In terms of surface roughness, while ST60 steel still outperformed the sintered specimens, the specimen sintered at 1200°C showed the closest surface finish to the reference material.

Acknowledgment

Laboratory of Metallurgy and Material Engineering, Department of Industrial Mechanical Engineering, Faculty of Vocation Studies, Sepuluh Nopember Institute of Technology.

References

[1] S. Kalpakjian and S. R. Schmid, *Manufacturing, Engineering and Technology*, 6th ed. Pearson Education, 2013.

[2] B. H. Amstead, P. F. Ostwald, and M. L. Begeman, *Teknologi Mekanik*. 1997: Erlangga, 1985.

[3] R. M. German, *Powder Metallurgy Science*. Princeton: Metal Powder Industries Federation, 1984.

[4] Z. Seikh, M. Sekh, G. Mandal, B. Sengupta, and A. Sinha, “Metal Matrix Composites Processed Through Powder Metallurgy: A Brief Overview,” *Journal of The Institution of Engineers (India): Series D*, 2024,

[5] “Powder Metal Technologies and Applications,” in *ASM Metal Handbook Volume 7*, ASM International, 1998.

[6] A. K. Sinha, *Powder Metallurgy*, 2nd ed. Dhanpat Rai & Sons, Nai Sarak, 110006, 1981. [Online]. Available: https://books.google.co.id/books?id=BfZlvZuWWIYC

[7] K. Rosika, A. Dian, and K. Djoko, “Pengujian Kemampuan XRF untuk Analisis Komposisi Unsur Paduan Zr-Sn-Cr-Fe-Ni,” *Prosiding Seminar Nasional Sains dan Teknologi Nuklir PTNBR– BATAN Bandung*, pp. 161–166, Jul. 2007.

[8] T. Febrianto, M. A. Zawawi, H. Seputro, and Mastuki, *Studi Eksperimen Pengaruh Tekanan Dan Suhu Sintering Terhadap Densitas Paduan Al-Mg Dengan Metode Metalurgi Serbuk*. Surabaya: Program Studi Teknik Mesin, Fakultas Teknik, Universitas 17 Agustus 1945 Surabaya, 2022.

[9] I. Setiyanto, “Pengaruh Variasi Temperatur Sintering Terhadap Ketahanan Aus Bahan Rem Sepatu Gesek,” Undergraduate Thesis, Universitas Muhammadiyah Surakarta, Surakarta, 2009.

[10] H. Nurrohman, “Pengaruh variasi temperatur dan waktu Holding Sintering terhadap Sifat Mekanik dan Morfologi Biodegradable Material Mg-Fe-Zn dengan Metode Metalurgi Serbuk untuk Aplikasi Orthopedic Devices,” pp. 107–107, 2017.

[11] I. Mufidah, “Pengaruh Pemanasan Serbuk Al Pra-Kompaksi Terhadap Sifat Fisis Komposit Al/SiC Hasil Metode Metalurgi Serbuk,” Undergraduate Thesis, Institut Teknologi Sepuluh Nopember, Surabaya, 2015.

[12] J. M. Capus, *Metal Powders: A Global Survey of Production, Applications and Markets*, 4th ed. Elsevier, 2005. Accessed: Aug. 22, 2025. [Online]. Available: https://books.google.co.id/books?hl=en&lr=&id=JBmPhh19k7AC&oi=fnd&pg=PR11&dq=Metal+Powders:+A+Global+Survey+of+Production,+Applications+and++Markets&ots=AphorH_xKv&sig=CL2j1v8tZNOcRYb53e42W8ox6O0&redir_esc=y#v=onepage&q=Metal%20Powders%3A%20A%20Global%20Survey%20of%20Production%2C%20Applications%20and%20%20Markets&f=false

[13] P. Hajikarimi, H. Shahsavari, M. Rahi, F. Sharif, and F. M. Nejad, “The Effect of Zinc Stearate Modification on Aging Characteristics of Asphalt Binder,” *IOP Conf Ser Mater Sci Eng*, vol. 416, p. 012083, Oct. 2018,

[14] R. Y. Syah, “Perancangan Punch & Dies Untuk Pembuatan Rangka Utama Sepeda ITS,” Undergraduate Thesis, Sepuluh Nopember Institute of Technology, Surabaya, 2016.

[15] *ASM Metals Reference Book*, Third Edition. ASM International, 1997.

[16] Mitutoyo, “SURFTEST SJ-410 Series,” in *M3 Solution Centers*, vol. 2196, 2015, pp. 1–7.

[17] I. D. N. Widarma, “Pengaruh Komposisi dan Ukuran Serbuk Leaching Agent NaCl Terhadap Sifat Mekanik dan Morfologi Biodegradable Material Mg-Fe-Zn Dengan Metode Metalurgi Serbuk Untuk Aplikasi Orthopedic Devices,” Undergraduate Thesis, nstitut Teknologi Sepuluh Nopember Surabaya, 2017.

[18] “Composites,” in *ASM Metal Handbook Volume 21*, ASM International, 2001.

[19] K. Herfurth and S. Scharf, “Casting,” in *Springer Handbook of Mechanical Engineering*, 2021, ch. 10, pp. 325–356.

[20] M. Zainuri, Y. Moniada, and D. Darminto, “Variasi tekanan dalam proses metalurgi serbuk dan pengaruhnya pada modulus elastisitas bahan komposit Al-SiC,” *Jurnal Fisika dan Aplikasinya*, vol. 1, no. 1, p. 050105, Jan. 2005,

[21] W. W. Wijaya, “Rancangan Alat Uji Tekan pada Bahan Komposit Natural Fiber Dengan Memperhatikan Aspek Keterulangan pada Hasil Pengujian,” Undergraduate Thesis, Universitas Sebelas Maret, Surakarta, 2011.

[22] “Mechanical Testing and Evaluation,” in *ASM Metal Handbook Volume 8*, ASM International, 2000.

[23] M. I. Almadani and R. Siswanto, “PROSES MANUFAKTUR MESIN POLES DAN AMPELAS UNTUK PROSES METALOGRAFI,” *JTAM ROTARY*, vol. 2, no. 1, p. 15, Apr. 2020,

[24] “Alloy Phase Diagrams,” in *ASM Metal Handbook Volume 3*, ASM International, 1992.